Tetrahedron Vol. 41, No. 11, pp. 2089 to 2098, 1985
Printed in Great Britain.

0040–4020/85 $3.00 + .00

THE ROLE OF INTERSYSTEM CROSSING STEPS IN SINGLET OXYGEN CHEMISTRY AND PHOTO-OXIDATIONS

NICHOLAS J. TURRO
Department of Chemistry, Columbia University, New York, NY 10027, U.S.A.

(*Received in Japan* 1 *May* 1984)

Abstract—Singlet oxygen chemistry and photo-oxidation reactions, in general, often require one or more critical reaction steps that involve an intersystem crossing from a singlet state to a triplet state or vice versa. This paper considers two important intersystem crossing mechanisms, electron spin–electron orbit (spin–orbit) coupling and electron spin–nuclear spin (spin–spin) coupling, and how they may be involved: (1) in the deactivation of $^1O_2$ to $^3O_2$; (2) in the thermal catalytic conversion of $^3O_2$ to $^1O_2$; and (3) in the fragmentation of aromatic endoperoxides to yield O_2 and an aromatic substrate.

From $O_2 + A$ *to* AO_2

This contribution is concerned with the intersystem crossing step that occurs in many systems involving oxidations with dioxygen. For a discussion of intersystem crossing mechanisms see Turro and Kraeutler.[1] We shall consider interactions of both $^3O_2$ ($^3\Sigma$) and $^1O_2$ ($^1\Delta$) with a substrate, A, in reactions which produce an oxidized product AO_2 and also certain examples of oxidized substrates which regenerate dioxygen upon thermolysis.

Scheme 1 summarizes a generalized and somewhat simplified treatment that reflects the point of view to be taken in systematizing analysis of our results. The substrate A may enter into an encounter with either $^3O_2$ or $^1O_2$ to form a loosely bound complex (C) or exciplex (X), respectively. Complex C may collapse to a diradical (D) via formation of a single bond from oxygen to A and X may collapse to a zwitterion (Z) via formation of a single bond from oxygen to A. (For simplicity, collapse of C to Z and X to D is omitted, but should be considered in a completely general analysis.)

From this scheme the key intersystem crossing steps are: (1) $^3C \rightleftarrows X$; and (2) $^3D \rightleftarrows {}^1Z$. We are interested in the structural and dynamical details of these steps and how they influence the observed reaction kinetics, reaction efficiencies and structures of products.

The role of the $^1O_2 \rightarrow {}^3O_2$ *deactivation process in the chemistry of singlet oxygen*

In general, whatever the mechanism or pathway for its production, $^1O_2$ will deactivate by either an irreversible chemical reaction with a substrate, A (Eq. 1), or via a pathway which results in the formation of $^3O_2$ (Eq. 2).

$$A + {}^1O_2 \xrightarrow{k_c} \text{chemistry} \qquad (1)$$

$$^1O_2 \xrightarrow{k_{ST}} {}^3O_2 \qquad (2)$$

Although, as written, the production of $^3O_2$ from $^1O_2$ is shown as an elementary step involving physical loss of electronic excitation energy, the detailed pathways

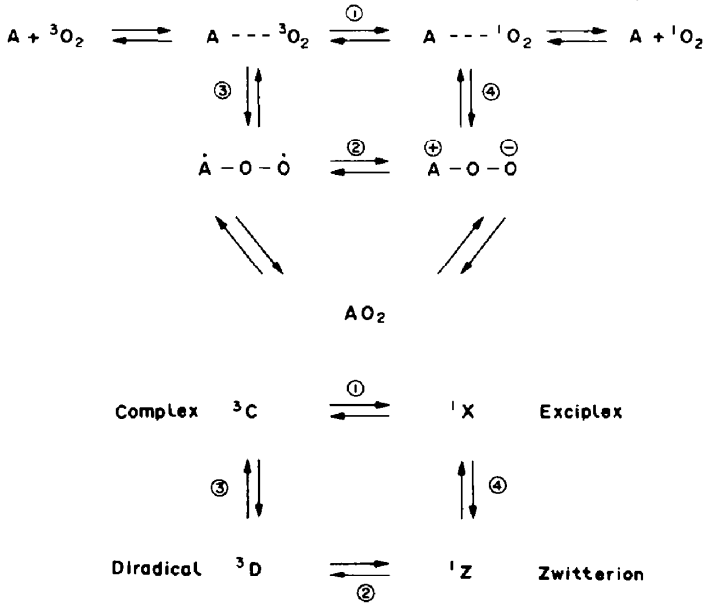

Scheme 1.

available for achievement of this overall process could be simple or complex. Among the pathways of greatest interest to chemists are: (a) a specific deactivation of $^1O_2$ by the substrate, A, Eq. (3); (b) a specific deactivation by a deliberately added or advantageous quencher, Q, Eq. (4); and (c) deactivation by solvent molecules, S, Eq. (5).

$$A + {}^1O_2 \xrightarrow{k_A} A + {}^3O_2 \quad (3)$$

$$Q + {}^1O_2 \xrightarrow{k_Q} Q + {}^3O_2 \quad (4)$$

$$S + {}^1O_2 \xrightarrow{k_S} S + {}^3O_2 \quad (5)$$

If we confine ourselves to consideration of conventional organic molecules for A, Q and S, there is no reason to expect that different fundamental mechanisms will occur for achieving Eqs (3), (4) or (5). Thus, all three are expected to fall within a common mechanistic framework. For simplicity, we can now view Eq. (2) as the sum of all processes, bimolecular, unimolecular, or pseudo unimolecular that bring about the overall process $^1O_2 \rightarrow {}^3O_2$. In this case:

$$k'_{ST} = k_A[A] + k_Q[Q] + k_S[S]. \quad (6)$$

The fact that the quencher concentration does not change (by definition of quencher) and that the solvent is in large excess allows reduction of Eq. (6) to Eq. (7):

$$k_{ST} = k_A[A] + k_d. \quad (7)$$

It should be pointed out that the phosphorescent emission of $^1O_2$ (Eq. 8), while technically critical for the direct measurement of the chemical and physical dynamics of $^1O_2$, does not contribute significantly to the measured decay dynamics of $^1O_2$. As a result, this step may be ignored in:

$$^1O_2 \xrightarrow{k_e} {}^3O_2 + h\nu. \quad (8)$$

The quantum efficiency for reaction of $^1O_2$ with A, based on unit efficiency of production of $^1O_2$ per photon absorbed is given by Eq. (9).

$$\Phi = \frac{k_c[A]}{k_c[A] + k_d + k_A[A]}. \quad (9)$$

In this case, the quantum efficiency of reaction of $^1O_2$ depends on three constants, k_c, k_A and k_d, and the concentration of A, Eq. (10).

$$\Phi = \frac{k_c[A]}{(k_c + k_A)[A] + k_d}. \quad (10)$$

In the limit of $k_d \ll (k_c + k_A)[A]$, the quantum efficiency is given by Eq. (11).

$$\Phi = \frac{k_c}{k_c + k_A} \quad \text{if } k_d \ll (k_c + k_A)[A]. \quad (11)$$

In the limits, $k_c \ll k_A$ and $k_d \gg (k_c + k_A)[A]$, the quantum efficiency is 0, Eq. (12).

$$\Phi = 0 \quad \text{if } k_c \ll k_A \text{ or if } k_d \gg (k_c + k_A)[A]. \quad (12)$$

From the above discussion it can be seen that, in order to obtain maximum efficiency of reaction of $^1O_2$ with A, knowledge of k_c, k_A and k_d is required along with knowledge of the factors that relate these quantities to the structures of A, Q and S. We have been interested in obtaining such knowledge in the hope and expectation that such information would lead to an understanding of the mechanism of the process by which $^1O_2$ may be produced by heating of $^3O_2$, Eq. (13).

$$^3O_2 \xrightarrow{k_{TS}} {}^1O_2. \quad (13)$$

In effect, steps 3–5 may be viewed as catalysed thermal deactivation of $^1O_2$ to $^3O_2$, each of which must possess a microscopic reversal, that is a catalysed thermal activation of $^3O_2$ to $^1O_2$. Of course, the 23 kcal/mol energy difference between $^1O_2$ and $^3O_2$ must be provided by heat from the reaction environment, but it should be noted that reactions with free energies of activation of the order of 30 kcal/mol proceed smoothly below 100°.

The possibility of achieving a method of thermally producing $^1O_2$ via a catalytic process rests on the design of a system that possesses a very small free energy of activation beyond the zero-point energy separation of $^3O_2$ and $^1O_2$. This design requirement suggests as one possibility a loose complex between $^3O_2$ and a template that can, with minimum entropy loss, provide a low energy pathway for intersystem crossing after the requisite state energy difference has been achieved.

In searching for true candidates two extreme situations are known in the literature. At one extreme is the chemically 'bound' form of singlet oxygen found in endoperoxides of aromatic hydrocarbons and, on the other hand, is the collision complex by which $^1O_2$ is deactivated by solvent molecules.

Rate limiting features in the deactivation of singlet oxygen

In analysing the mechanism of intersystem crossing between the lowest singlet and triplet states of molecular oxygen, one comes into contact with the problem of deciding whether electronic relaxation, vibrational relaxation or spin relaxation is rate determining.[2] We shall consider each possibility in turn.

Electronic interactions. If electronic interactions are rate determining in a radiationless, electronic state interconversion, one may employ the method of orbital interactions to establish, qualitatively, the most favourable geometry for electronic interactions.[3] The lowest energy pathways for chemical reactions and radiationless electronic transitions are determined by molecular geometries for which the overlap of the highest occupied (HO) molecular orbital and the lowest unoccupied (LU) molecular orbital is most favoured. For molecular oxygen we are concerned with two electronic configurations corresponding to the $^1\Delta$ ($^1O_2$) and the $^3\Sigma$ ($^3O_2$) states (Fig. 1, top):

$$^1\Delta = K(\pi^*_{xz})^2(\pi^*_{yz})^0$$

$$^3\Sigma = K(\pi^*_{xz})^1(\pi^*_{yz})^1$$

where K refers to the core spin paired orbitals and where the O–O axis is taken in the z-direction. Since π^*_{xz} and π^*_{yz} both have two nodal planes (one containing the O–O axis and one perpendicular to this), both the HO (π^*_{xz}) and the LU (π^*_{yz}) orbitals have identical orbital symmetry properties.

For confirmation let us consider the interaction of an ethylene with the $^1\Delta$ state. Let us fix the molecular plane of the ethylene parallel to the x–y plane and place the

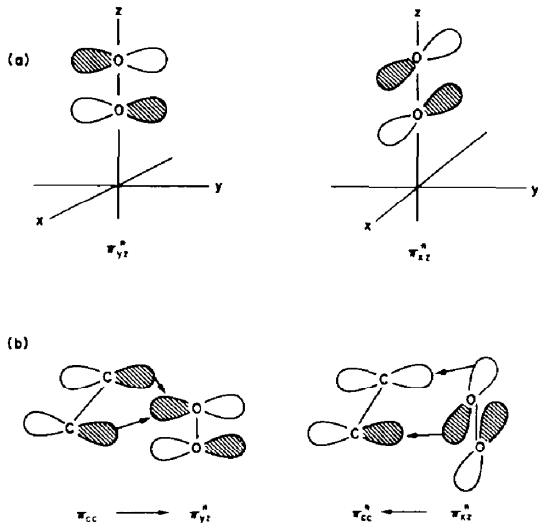

Fig. 1. Definition of an axis system for the nodal properties of the π^* orbitals of molecular oxygen (top). For the 1Δ state of oxygen, the π^*_{yz} orbital is defined as the LU and the π^*_{xz} orbital the HO. The lower portion of the figure shows the modes of HO–LU interactions between $^1\Delta$ state of an ethylene. (a) Definition of oxygen orbitals; (b) Charge transfer orbital interactions.

C–C axis parallel to the x-axis (Fig. 1, bottom). An analysis shows that a geometry approaching a perepoxide structure leads to the most favourable orbital interaction. In this geometry the charge transfer $\pi_{CC} \rightarrow \pi^*_{yz}$, and the $\pi^*_{xz} \rightarrow \pi^*_{CC}$ interactions are favourable (positive overlap), i.e. the HO of the ethylene can effectively interact with the terminus of the LU of the $^1\Delta$ state of molecular oxygen, and the HO of the oxygen can effectively interact with the terminus of the LU of the ethylene because these interacting MOs have the same symmetry with respect to the bisecting plane.

Accordingly, the $^1\Delta$ state of molecular oxygen is expected to approach the double bond of an ethylene via a geometry involving a trigonal ring of the two unsaturated C atoms and a single O atom 'tailed' by the second O atom which lies roughly perpendicular to the plane of the CCO ring. Continuing with this reasoning, if the radiationless $^1\Delta \rightarrow {}^3\Sigma$ transition is rate limited by the most favourable electronic interactions, collisions of an ethylene and $^1O_2$ which possess this geometry will be most effective at causing the $^1O_2 \rightarrow {}^3O_2$ deactivation.[4]

Vibrational interactions. For the vast majority of chemical reactions vibrational relaxation is rarely rate limiting. Although there are a large number of examples of vibration relaxation limited processes involving relaxation of electronically excited states, most involve systems at low temperature and/or in rigid environments. Experimental hallmarks of a vibration relaxation limited process are the observation of exceptionally large isotope effects, a decrease in rate with an increase in the electronic energy gap between the states involved in the transition, and an increase in the rate of relaxation as the frequency of the interacting vibration.[5] The simplest explanation of these results is that vibrational energy is best removed by large energetic chunks: (1) as the electronic energy gap involved in the transition increases the total vibrational energy to be removed is increased and the rate of the radiationless transition slows down; (2) as the frequency of the interacting vibration increases, the energy that a given vibration is able to remove (per quantum) increases and the rate of the radiationless transition speeds up; and (3) as a heavy isotope is substituted for a light isotope, the frequency of the corresponding vibration decreases, so as in (2), above, the rate of the radiationless transition decreases.

Magnetic interactions. If magnetic interactions are rate determining in a radiationless relaxation very unusual structure effects on reaction rates can be observed. The reason for this behaviour is that the common mechanisms by which magnetic effects can cause rates to vary depend on electron spin–electron orbit interaction and electron spin–nuclear (hyperfine) spin interaction.[1] The selection rules which determine favourable situations for spin–orbit interactions and spin–spin interactions are quite different from the selection rules which determine favourable electronic or vibration interactions.[6]

Whatever the mechanism of intersystem crossing, the molecular system under examination must achieve a geometry for which a singlet state and triplet state have similar energies or, most favourably for intersystem crossing, energies which are small compared to the magnetic interaction inducing intersystem crossing. Singlet and triplet states of molecules possessing only first row atoms have small energy differences for geometries corresponding to surface crossings or surface touchings.[7] Common examples of reactions for which triplet and singlet surfaces generally come close in energy are ground state forbidden pericyclic reactions and cleavage of single bonds. In the former case, the geometry corresponding to the transition state may be classified as a diradicaloid. An important property of diradicaloids is that they commonly possess schizophrenic electronic properties because at the diradicaloid geometry state mixing of diradical (D) and zwitterionic (Z) structures is often facile.[7]

At the diradicaloid geometry spin–orbit interactions or spin–spin interactions can operate to induce intersystem crossing.[6] To a good approximation, as a rule spin–orbit coupling is favoured when a transition between D and Z states can occur and when the electronic transition between D and Z states contains a component corresponding to a one-centred orbital transition between orthogonal p orbitals. Figure 2 shows schematically how this rule comes about. In order to create angular momentum an orbital transition must involve orbitals whose axes are orthogonal to each other and to the axis around which the orbital angular momentum is being created. The rotation of a p_x orbital about the z-axis creates angular momentum about this axis. Thus, a $p_x \rightarrow p_y$ orbital transition, which corresponds to rotation of p_x about the z-axis, creates angular momentum along the z-axis. The spin–orbit operator, H_{SO}, may be viewed as the force that creates the electronic angular momentum. In a very schematic form Fig. 2 represents the quantum mechanical matrix element $\langle p_x|H_{SO}|p_y\rangle$ which is a measure of the spin–orbit interaction. Multiplication of p_x by H_{SO} corresponds to the rotation of p_x by 90° along the z-axis, i.e. $\langle p_x|H_{SO}| \rangle = p_y$. Thus, $\langle p_x|H_{SO}|p_x\rangle = 0$ and $\langle p_y|H_{SO}|p_y\rangle = 0$. From this qualitative analysis, $p_x \rightarrow p_y$ transitions on the same atomic centre can be seen to lead to the maximal value of spin–orbit matrix

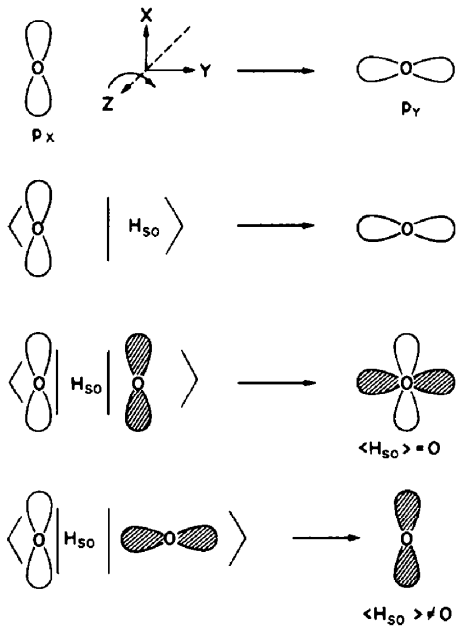

Fig. 2. Schematic representation of spin–orbit coupling on a single atomic centre. See text for discussion.

element and, hence, to the most favourable situation for spin–orbit induced intersystem crossing.

The take-home message from this analysis is that favourable geometries for intersystem crossing can be found for systems which achieve the following conditions along a reaction pathway: (1) a geometry corresponding to a diradicaloid, because at this geometry singlet and triplet states will come close in energy and because D and A mixing is generally significant at diradical geometries; and (2) a D → Z (or Z → D) transition which possesses a significant component that corresponds to a $p_x \rightarrow p_y$ transition on a single atomic centre.

The second mechanism for intersystem crossing, electron–nuclear hyperfine coupling is generally so weak that the singlet and triplet states involved in intersystem crossing must be degenerate (or very nearly degenerate) and persist in this condition for a nanosecond or longer.[1,8] Such a situation will arise for diradicals and for radical pairs which possess very weak electronic exchange. For such situations, even the very weak magnetic moments of nuclei can exert sufficient magnetic forces on electronic spin to cause intersystem crossing.

Some general observations concerning the physical and chemical quenching of $^1O_2$

The bimolecular quenching of $^1O_2$ by a substrate A may be classified empirically as chemical if a net reaction between $^1O_2$ and A occurs and physical if there is no net reaction. The latter may be described mechanistically as chemically reversible quenching or vibrational quenching. The temperature dependence of the rate constants for chemical quenching of $^1O_2$ show that the kinetics of these reactions are dominated by entropies of activation and possess enthalpies of activation that generally are of the order of 0 ± 1 kcal/mol.[9] The physical quenching of $^1O_2$ shows a remarkable and general deuterium isotope effect.[10] The deuterium effect is quite remarkable in magnitude and specificity. For example, the lifetime of $^1O_2$ in deuterated solvents (e.g. $CDCl_3$, CD_3CN, D_2O) is typically 10 times longer than in the corresponding protiated solvents.

The entropic control of the rate of reaction of $^1O_2$ has been interpreted in terms of a reversibly formed complex between $^1O_2$ and the substrate,[11] with the complex having very strict structural requirement for proceeding to products. Such a situation is analogous to the situation postulated for the substrate catalysed

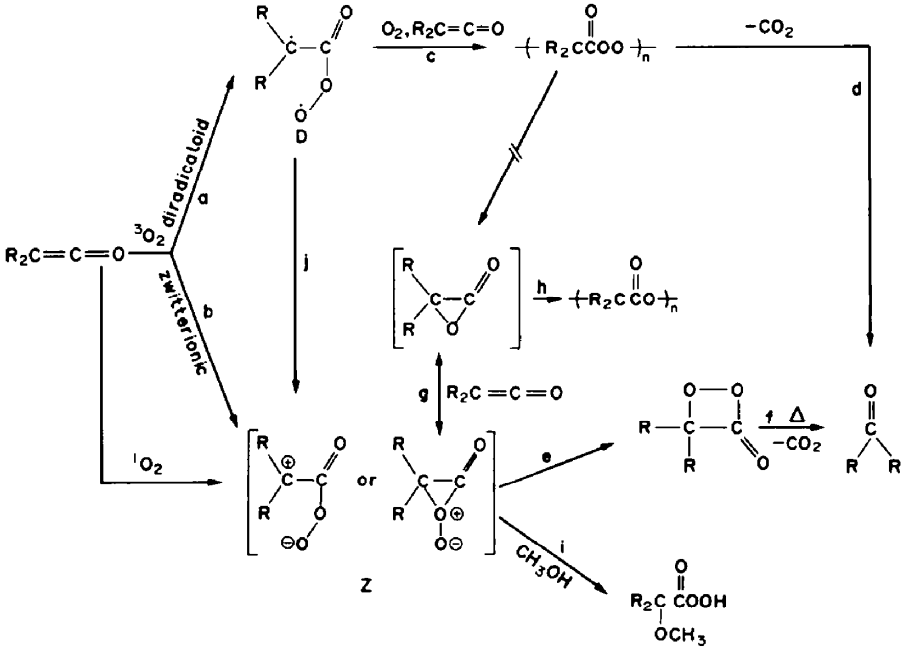

Scheme 2.

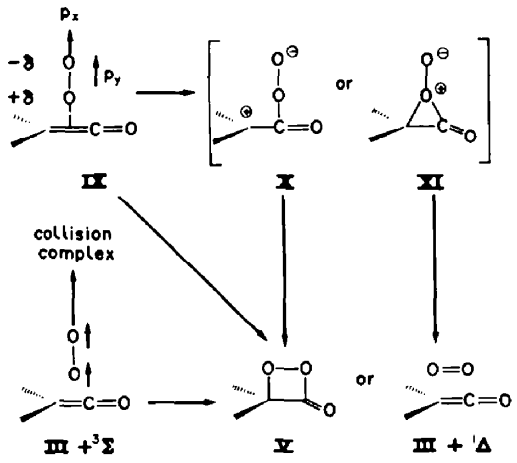

Scheme 3.

intersystem crossing of $^3O_2$ to $^1O_2$. Following this line of reasoning it is to be expected that there could be a substantial deuterium isotope effect on the thermally catalysed intersystem crossing of $^3O_2$ to $^1O_2$ and that the vibrational quenching of $^1O_2$ could have strict steric requirements.

Reaction of dioxygen with ketenes

The reaction of dioxygen with ketenes may be interpreted in terms of Scheme 1. Dimethyl ketene (DMK) and diphenyl ketene (DPK) both undergo thermal auto-oxidation with $^3O_2$, but produce completely different products (Eqs 14 and 15).[12]

$$(CH_3)_2C{=}C{=}O + {}^3O_2 \rightarrow \{(CH_3)_2C(O)O\}_n \quad (14)$$

$$Ph_2C{=}C{=}O + {}^3O_2 \rightarrow \{Ph_2C(O)\}_n + Ph_2C{=}O \quad (15)$$

The auto-oxidation of DMK is postulated to yield a diradical D (Scheme 2) which initiates a polymerization that generates a polyperester. Zwitterionic (Z) intermediates are ruled out by the lack of trapping of Z species when the auto-oxidation is run in the presence

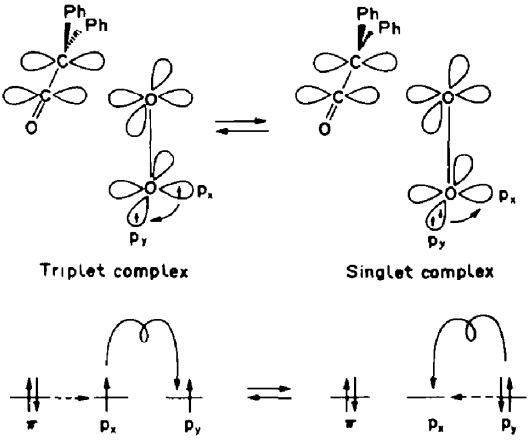

Scheme 4.

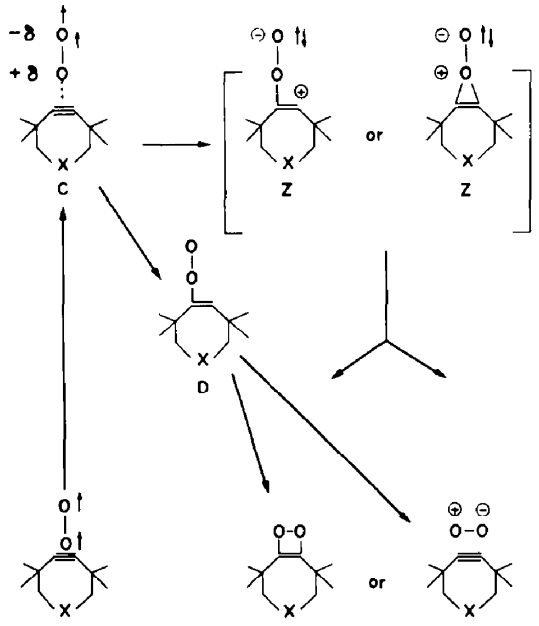

Scheme 5.

of zwitterion traps such as sulphides. In contrast, the auto-oxidation of DPK is completely inhibited by the addition of methanol and an α-methoxy peracid, the expected product from trapping of Z, is formed. Indeed, the same products are formed when DPK reacts with $^1O_2$.

Triplet oxygen is a textbook example of a diradical, yet zwitterionic intermediates are implicated in its reaction of DPK. We propose that a $^3D \rightarrow {}^1Z$ or a $^3C \rightarrow {}^1X$ intersystem crossing (Scheme 1) occurs in the reaction of DPK and $^3O_2$. Several possible detailed pathways are shown in Scheme 3.

From the discussion of orbital interaction, it is suggested that the favoured geometry is that shown in Scheme 4, i.e. a geometry for which a single centred $p_x \rightarrow p_y$ orbital jump can occur, as required for favourable spin–orbit interactions, as shown in Fig. 2.

Reactivation of dioxygen with strained acetylenes

Nearly a decade ago we reported that reaction of $^3O_2$ and $^1O_2$ were driven by the desire to design a catalytic system that could produce $^1O_2$ from $^3O_2$ by simple heating, by the desire to design syntheses of 1,2-dioxetenes and by the desire to uncover an understanding of the mechanisms of singlet–triplet conversion in oxidation reactions.

Nearly a decade ago we reported that reaction of $^3O_2$ and $^1O_2$ with certain strained acetylenes lead to chemiluminescence.[13] Analysis of the results indicated the occurrence of an oxygen–acetylene intermediate (Scheme 5) or free singlet oxygen on the chemiluminescence pathway. The possible generation of free singlet oxygen by decomposition of an oxygen–acetylene intermediate represents a catalytic generation of $^1O_2$ from $^3O_2$. The mechanism for the key step for spin inversion can be envisaged as being analogous to that shown in Scheme 4 for the reaction of oxygen with ketenes.

The investigation of reactions of strained acetylenes with $^3O_2$ and $^1O_2$ were driven by the desire to design a catalytic system that could produce $^1O_2$ from $^3O_2$ by simple heating, by the desire to design syntheses of 1,2-dioxetenes and by the desire to uncover an understanding of the mechanisms of singlet–triplet conversion in oxidation reactions.

Further investigation of these systems by Krebs and Schmalstieg[14] suggested that the chemiluminescent

pathway is a minor pathway in the reaction of $^1O_2$ and strained acetylenes. Indeed, the reaction of $^1O_2$ with **1** leads predominantly to oxidation of the sulphide and not to reaction with the triple bond. Colberg *et al.*[15] demonstrated that the major pathway for reaction of $^3O_2$ with strained acetylenes is a chain auto-oxidation. Thus, the chemiluminescence pathway is not quenched by typical radical scavengers (hindered phenols), but is quenched by olefins known to react with singlet oxygen.

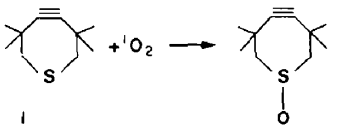

(16)

1

The possible complicating factors introduced by the occurrence of a sulphur atom in **1**, led us to search for a simple hydrocarbon system that might be capable of reacting with both $^1O_2$ and $^3O_2$. We selected cyclo-octyne as a moderately strained (25 kcal/mol) acetylene which might have these desired properties and we were encouraged by a report that a petroleum ether solution of cyclo-octyne undergoes auto-oxidation on standing in air.[16] In refluxing benzene, we found that auto-oxidation of cyclo-octyne leads to cyclo-octanedione as the product (Eq. 17). Chemiluminescence, much weaker

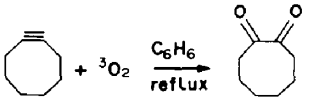

(17)

than that observed during the auto-oxidation of cycloheptyne derivatives, was observed.[17]

Reaction of $^1O_2$ (under these conditions such that auto-oxidation is negligible) with cyclo-octyne also leads to formation of 1,2-cyclo-octanedione as the major

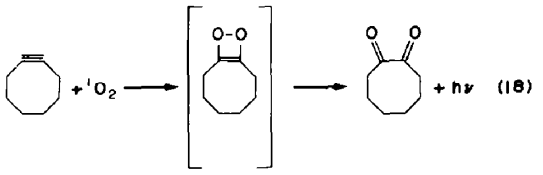

(18)

product (Eq. 18). In this case a readily observed chemiluminescence, experimentally identical to photo-excited fluorescence of 1,2-cyclo-octanedione is observed during the course of the reaction. Two types of experiments confirmed the involvement of $^1O_2$ as the oxidizing species responsible for the chemiluminescence.[17] (1) The chemiluminescence intensity was *ca* 10 times greater when reaction was run in $CDCl_3$ relative to $CHCl_3$. (2) The Stern–Volmer constants for quenching of chemiluminescence by olefins were in precisely the same ratio as the constants for quenching of $^1O_2$ by the same olefins.

An oxetene intermediate is proposed for the precursor of the excited 1,2-cyclo-octanedione which is responsible for the observed chemiluminescence. Photo-oxidation at −78° demonstrated the production of an intermediate(s) which produce chemiluminescence upon warm-up. However, attempts to structurally characterize this intermediate(s) by low temperature NMR or IR failed.

Thermolyses of endoperoxides of aromatic compounds

Thermolyses of many endoperoxides of aromatic compounds generate molecular oxygen and the parent aromatic species often in quantitative yield (Eq. 19).[18] A fascinating feature of these reactions is the observation of singlet molecular oxygen as a product of the thermolyses. The thermolyses of endoperoxides **1–4** all follow clean first-order kinetics (appearance of aromatic followed by UV spectroscopy).[19] The

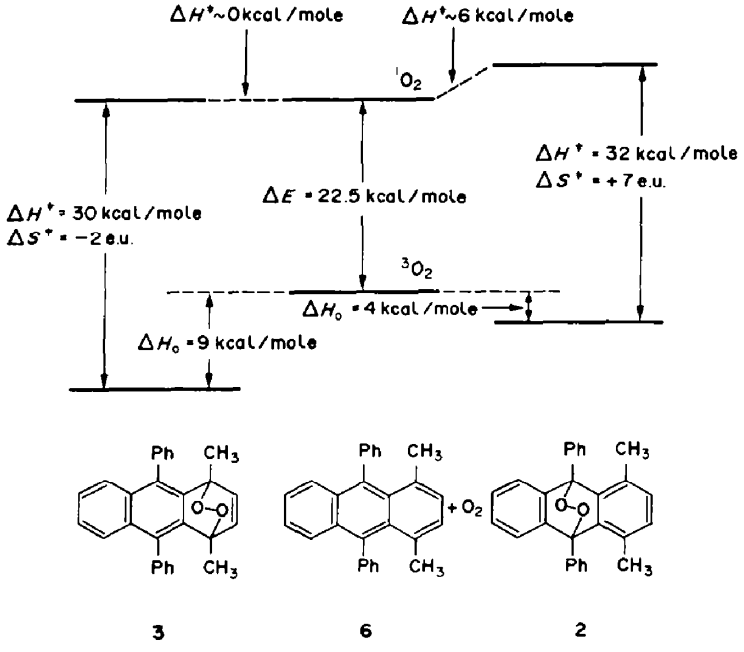

3 **6** **2**

Fig. 3. Thermochemical and activation parameters for the thermolyses of endoperoxides **2** and **3**.

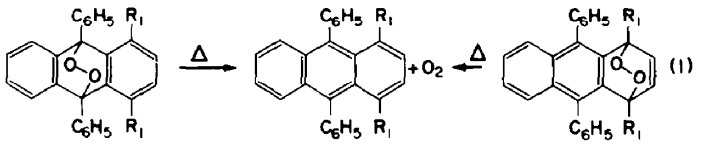

(19)

1 R_1 = H
2 R_1 = CH_3
5 R_1 = H
6 R_1 = CH_3
3 R_1 = CH_3
4 R_1 = OCH_3

activation parameters, derived from the temperature dependence of the first-order rate constants are summarized in Fig. 3 and Table 1. The yields of $^1O_2$ were determined by chemical trapping and the reaction enthalpies were measured by differential scanning calorimetry (solid state). The values obtained were similar in magnitude to those obtained from measurement of $\Delta H‡$ and the assumption of 0 kcal/mol of activation energy for addition of $^1O_2$ to the aromatic species.

From the activation parameters and $^1O_2$ yields, two distinct and potentially competing mechanisms were postulated (Scheme 6): (1) cleavage of the C—O bond to produce a singlet diradical intermediate capable of fragmenting to $^1O_2$ or of intersystem crossing to yield a triplet diradical capable of fragmenting to $^3O_2$; and (2) a concerted pathway in which both C—O bonds are broken synchronously (although not necessarily at the same rate) to yield $^1O_2$.

If pathway (1) is followed, then $\Delta S‡$ is expected to be

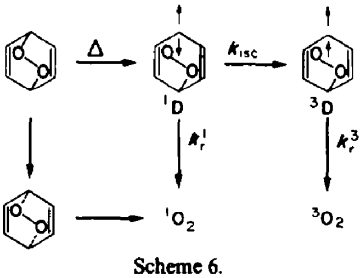

Scheme 6.

of a magnitude typical for formation of a diradical, whereas if pathway (2) is followed, then $\Delta S‡$ is expected to be of a magnitude typical of concerted pericyclic reactions. Inspection of the literature shows that a value ($\Delta S‡ = 9$ e.u.) is typical of molecule → diradical reactions (e.g. the thermolysis of cyclobutane) (Scheme 7), whereas a value of $\Delta S‡ = 0$ e.u. is typical of

Table 1. Activation parameters, singlet oxygen yields and reaction enthalpies for thermolyses of endoperoxides[a]

Endoperoxide	$\Delta H‡$ (kcal/mol)	$\Delta S‡$ (e.u.)	% $^1O_2$	ΔH (kcal/mol)
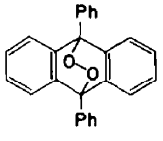	32	10	32	6
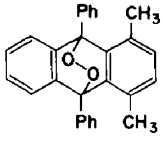	32	7	50	4
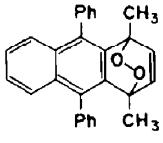	30	−2	92	9
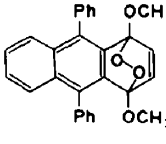	24	0	95	2

[a] 1,4-Dioxane solvent.

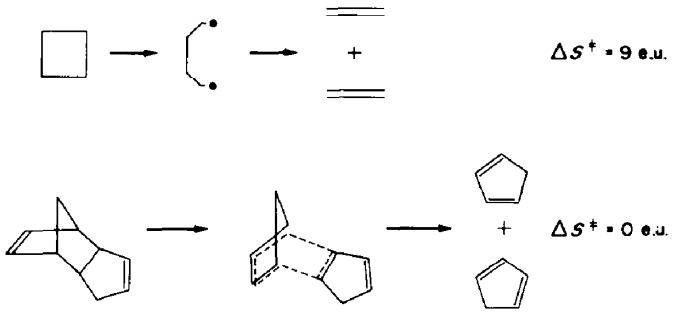

Scheme 7.

concerted reactions (e.g. the thermolysis of endodicyclopentadiene, Scheme 7).

On the basis of the postulate that an endoperoxide decomposes predominantly by either the diradical pathway (1) or by the concerted pathway (2), the thermolyses of 9,10-anthracene endoperoxides are readily classified as diradical reactions, whereas the thermolyses of 1,4-anthracene endoperoxides are classified as concerted reactions, i.e. a correlation between $^1O_2$ yields and $\Delta S\ddagger$ exists and this correlation allows mechanistic distinctions to be made.

Magnetic field and magnetic isotope effects on the generation of $^1O_2$

Of the postulated mechanisms for thermolyses of endoperoxides, the diradical mechanism (pathway 1) may be influenced by applied laboratory magnetic fields, whereas the concerted mechanism (pathway 2) should not be influenced by applied laboratory magnetic fields. The rate of singlet–triplet crossing (k_{ST}) from ^1D to ^3D is expected to depend to some extent on the strength of applied laboratory fields.[20] This dependence arises because, for strong enough external fields, k_{ST} for a diradical possessing degenerate (or nearly degenerate) singlet and triplet levels will be proportional to ΔgH, where Δg is the difference in g factors at the two radical centres and H is the strength of the applied field. The magnitude of Δg is expected to be substantial (*ca* 0.01) for a diradical possessing a peroxy and a carbon radical centre.[8,21] Typical values of Δg for two carbon-centred radicals are *ca* 0.001. As an order of magnitude approximation, if $\Delta g \sim 10^{-2}$ and $H \sim 10{,}000$ G, the values of $\Delta gH \sim 10^8\ s^{-1}$. The rates of decay of diradicals are of this order so that, from Scheme 6 it is conceivable that the yield of $^1O_2$ from thermolysis of anthracene 9,10-endoperoxides may be magnetic field dependent. However, the yield of $^1O_2$ from anthracene 1,4-endoperoxides (concerted reaction) should not be magnetic field dependent, and the $^1O_2$ yield should remain constant as H increases. These qualitative expectations are in full agreement with the data in Table 2 and Fig. 4.

A magnetic isotope can speed up the $^1D \rightarrow {}^3D$ intersystem crossing in the same manner as an external magnetic field.[8,21] Thus, as shown schematically in Fig. 5, if the diradical pathway is followed, the yield of $^1O_2$ will be smaller for endoperoxide molecules containing ^{17}O (a magnetic isotope) than for endoperoxides containing $^{16}O/^{18}O$ (non-magnetic isotopes). A corollary is the experimental expectation that, if $^1O_2$ produced by thermolysis is trapped selectively and quantitatively as the reaction occurs, the (untrapped) $^3O_2$ produced will be enriched in ^{17}O!

Table 2. Yield of $^1O_2$ formation and isotopic effect in the thermolysis of **1**

% yield of $^1O_2$[a]				
^{16}O[b]	$^{17,18}O$[c]	^{18}O[d]	Magnetic field	Solvent
37±1	34±1	37±1	0.5 G	$CHCl_3$
32±2	31±1	31±1	10 kG	$CHCl_3$
32±1	28±1	32±2	0.5 G	Dioxane
27±2	23±1	28±2	12 kG	Dioxane
28.3±0.3	27.2±0.2	28.4±0.2	0.5 G	Benzene
27.8±0.8	27.8±0.7	28.1±0.8	10 kG	Benzene

[a] The yield of $^1O_2$ is defined as the ratio of disappearance of tetracyclone to the appearance of **5**. The yield is derived directly from the mixed isotopic oxygen containing **1** employed; i.e. no adjustment in yield is made for the differing percentages of ^{16}O, ^{17}O and ^{18}O in the starting material, **1**. The error given is the standard deviation derived from a minimum of eight independent samples measured once.

[b] The initial isotopic composition is 99.8% ^{16}O, i.e. natural abundance oxygen.

[c] The initial isotopic composition is 60% ^{18}O and 37% ^{17}O (and 3% ^{16}O).

[d] The initial isotopic composition is 92% ^{18}O and 4% ^{17}O (and 4% ^{16}O).

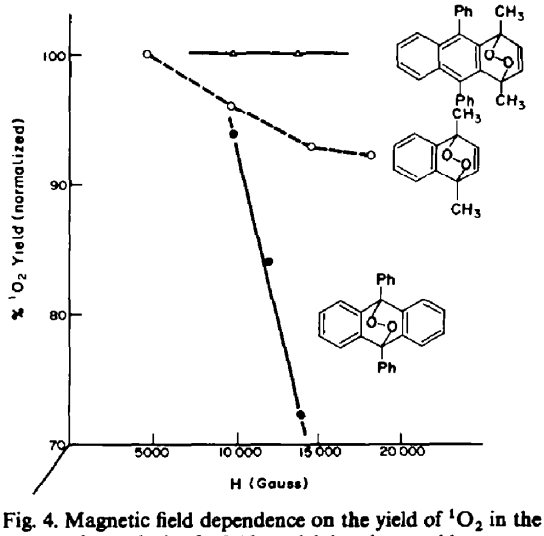

Fig. 4. Magnetic field dependence on the yield of $^1O_2$ in the thermolysis of a 9,10- and 1,4-endoperoxide.

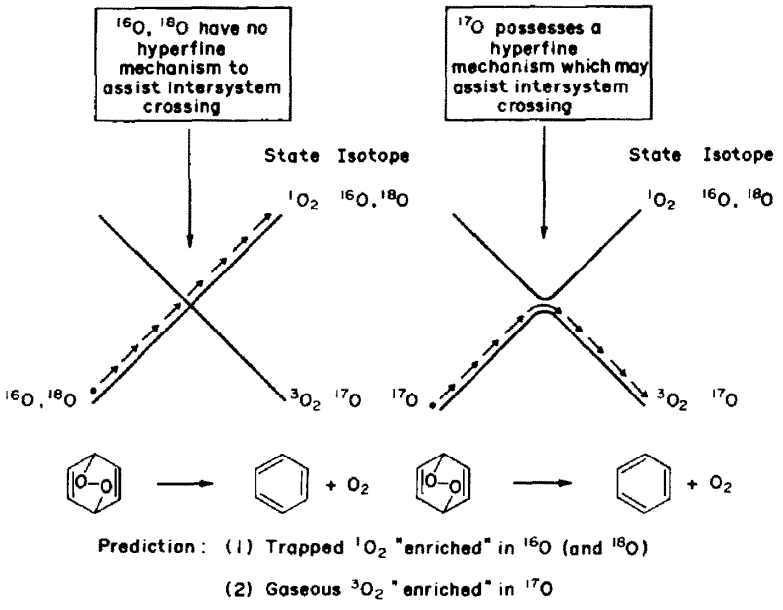

Fig. 5. Schematic description of the basis of a magnetic isotope effect on the thermolysis of an endoperoxide by the diradical mechanism shown in Scheme 6.

Both of these expectations were confirmed experimentally each by an independent type of measurement:[19] (a) the ^{17}O and ($^{16}O+^{18}O$) content of untrappable oxygen was analysed by mass spectrometry; and (b) the yield of trapped $^1O_2$ was evaluated by quantitative determination of the amount of reacted acceptor, when 1-$^{16}O_2$, 1-$^{18}O_2$ or 1-$^{17}O_2$-37% were employed. From Table 3 it can be seen that the yield of $^1O_2$ formation is smaller for 1-$^{17}O_2$-37% than for 1-$^{16}O_2$ or 1-$^{18}O_2$. The fact that both 1-$^{16}O_2$ and 1-$^{18}O_2$ produce the same yield of $^1O_2$, while 1-$^{17}O_2$-37% produces less rules out a significant mass isotope effect as the basis for different yields. Furthermore (Table 3), we observed that the results changed quantitatively when reactions were run in a laboratory magnetic field, a result which confirms the conclusion that a magnetic spin isotope effect was operating.

Since the amount of reacted trap is monitored in the yield measurements, they only provide an indirect test of the isotopic enrichment. A direct measurement involves determination of the isotopic composition of the untrappable molecular oxygen produced in the thermolysis of 1-O_2. Table 3 lists the isotopic composition of untrapped molecular oxygen produced from thermolysis of 1-O_2 in $CHCl_3$ and in dioxane. The results demonstrate that the untrappable molecular oxygen is indeed enriched in ^{17}O relative to the control sample which contained $<37.0\%$ of ^{17}O.

Table 3. ^{17}O composition of nontrappable O_2 generated from the thermolysis of endoperoxide

Endoperoxide	^{17}O composition	Magnetic field	Solvent
1[a]	38.0±0.5	0.5 G	$CHCl_3$
	36.8±0.2	10 kG	$CHCl_3$
	37.6±0.1	0.5 G	Dioxane
	37.6±0.2	12 kG	Dioxane
	36.9±0.1	0.5 G	Benzene
	36.9±0.1	10 kG	Benzene

[a] In the presence of tetracyclone.

Relationships between the thermolysis of endoperoxides and the reaction of molecular oxygen with aromatic compounds

An interesting question arises concerning the relationship of the [4+2] cycloaddition reaction of $^1O_2$ with aromatic compounds and the [4+2] retrocycloaddition reaction of aromatic endoperoxides.[2] From information in the literature[9] $\Delta H‡$ is 0±1 kcal/mol for the quenching of $^1O_2$ with a wide variety of substrates. The differences in the quenching rate constants for $^1O_2$ are dominated by the $\Delta S‡$ term. The reactions of $^1O_2$ with dienes and aromatic compounds are generally considered to be concerted [4+2] cycloadditions (although the occurrence of perepoxide and/or related intermediates may be involved in certain cases). If the thermolysis of an aromatic endoperoxide to produce $^1O_2$ is the microscopic reverse of the reaction of $^1O_2$ with the corresponding aromatic compound, there is essentially no activation for the reverse reaction, and the value of ΔH for the reactions can be evaluated from knowledge that 22.5 kcal/mol of energy is required to produce $^1O_2$ from $^3O_2$ and the activation enthalpy for thermolysis of the endoperoxide $\Delta H_{AO_2}‡ - 22.5$ kcal/mol $= \Delta H$.

From our data (Table 1), $\Delta H‡$ for the endoperoxide **1** is 32±2 kcal/mol. Thus, if thermolysis of **1** proceeds by a concerted reaction that is the microscopic reverse of the addition of $^1O_2$ to **5**, the value of 10±2 kcal/mol is computed for the reaction enthalpy. This value is within the error of the value of $\Delta H = 13\pm5$ kcal/mol for the photo-oxidation of **5**.

With the assumption that values of ΔH measured for solid-phase thermolysis are adequate for a discussion of the solution thermolyses, the competition between concerted one-step and diradical two-step mechanisms may be considered in the context of the microscopic

relationship between the thermolysis and the addition of $^1O_2$ to anthracenes. Since the value of $\Delta H\ddagger$ for the quenching of $^1O_2$ by a wide range of structures is 0 ± 1 kcal/mol, values of ΔH for the thermolysis may be calculated on the basis of the assumption of microscopic reversibility. In this regard, the thermochemical data for the thermolysis of **3** and **4** is fully consistent with the thermolysis as the microscopic reverse of the addition of $^1O_2$ to the pertinent anthracenes.

On the other hand, thermochemical data for the thermolysis of **1** and **2** are consistent with a diradical mechanism, although this need not be the exclusive pathway, i.e. the data are also consistent with a competition between concerted and diradical mechanisms. Furthermore, the basic assumption of microscopic reversibility demands that identical reactants and products are involved in the individual elementary chemical step under analysis. Since the thermolyses of **1** and **2** produce **5** and **6**, singlet molecular oxygen and triplet molecular oxygen, the products are different from the reactants for photo-oxidation of **5** and **6**, i.e. **5** and **6** and singlet molecular oxygen only. Thus, the thermolysis of **1** and **2** and the concerted photo-oxidation of **5** and **6** are not related by microscopic reversibility.

The free energy difference between concerted and diradical pathways is of the order of several kilocalories per mole. Evidently, the diradical pathway requires a slightly higher enthalpy of activation than the concerted pathway, but enjoys a more favourable activation entropy. Both cycloelimination pathways, furthermore, compete with a third process, the cleavage of the O—O bond. In the case of unsubstituted anthracene, the latter process dominates.

The results of our studies allow a number of insights to the mechanism of the fragmentation of endoperoxides into molecular oxygen and an aromatic compound, and to the mechanism of addition of molecular oxygen to aromatic compounds. There are two mechanisms by which the fragmentation occurs: a diradical mechanism involving the initial homolytic cleavage of a single C—O bond followed by eventual loss of O_2 (in a singlet or triplet state) and a mechanism involving the concerted cleavage of both C—O bonds. The primary yield of singlet oxygen is relatively low in the diradical mechanism and is nearly quantitative in the concerted mechanism. It is remarkable that for 1,4-endoperoxides nearly all of the activation energy for reaction is taken up in producing electronic excitation for the singlet oxygen produced. Thus, in spite of the fact that the overall reaction—endoperoxide $\rightarrow$ $^1O_2$ + aromatic compound—is strongly endothermic, the efficiency of the chemiexcitation process is exceptionally high. It is important to note that these results lead to the conclusion that activation energy can indeed be channelled efficiently into electronic excitation energy, a possibility that has been the subject of some discussion in the literature.

Magnetic field and magnetic isotope effects provide a novel means to test for reactions involving diradicals. Although a discussion of the theoretical details of the origin of these effects are beyond the scope of this paper, it is interesting to note that the exchange interaction between the odd electrons of the postulated diradical (Scheme 6) is not sufficient to completely suppress hyperfine-induced intersystem crossing. It follows that, if the exchange interaction can be reduced, even larger ^{17}O isotope may be observed. It also follows that an enhanced exchange may completely suppress the ^{17}O isotope effect. The latter situation may explain the failure to observe ^{17}O enrichment when benzene is employed as solvent (Table 3).

CONCLUSION

The structural requirements for intersystem crossing in reactions of singlet oxygen in the radiationless deactivation of singlet oxygen and in the thermolysis of endoperoxides that produce singlet oxygen have been explored. These ideas can be employed to gain an understanding of the important, yet unusual and fascinating, role played by molecular oxygen in photo-oxidations.

Acknowledgements—The author wishes to thank the National Science Foundation and the Air Force Office of Scientific Research for their generous support of this research.

REFERENCES

[1] N. J. Turro and B. Kraeutler, *Diradicals* (Edited by E. T. Borden), p. 259. Wiley, Chichester (1982).
[2] D. R. Kearns, *J. Am. Chem. Soc.* **91**, 6554 (1969); *Chem. Rev.* **71**, 395 (1971).
[3a] S. Inagaki, S. Yamabe, H. Fujimoto and K. Fukui, *Bull. Chem. Soc. Jpn* **45**, 2510 (1972); [b] K. Okubo and H. Sato, *Ibid.* **53**, 533 (1980).
[4] P. B. Merkel and D. R. Kearns, *J. Am. Chem. Soc.* **94**, 7224 (1972).
[5] N. J. Turro, *Modern Molecular Photochemistry*, Chap. 6. Benjamin, Menlo Park (1978).
[6a] L. Salem and C. Rowland, *Angew. Chem. Int. Ed. Engl.* **11**, 92 (1971); [b] L. Salem, *Pure Appl. Chem.* **33**, 317 (1973).
[7a] J. Michl, *Top. Cur. Chem.* **46**, 1 (1974); [b] W. G. Dauben, L. Salem and N. J. Turro, *Acc. Chem. Res.* **8**, 41 (1975).
[8] N. J. Turro, *Proc. Natl. Acad. Sci. U.S.A.* **80**, 609 (1983).
[9a] J. R. Hurst and G. B. Schuster, *J. Am. Chem. Soc.* **104**, 6854 (1982); [b] A. A. Gorman, G. Lovering and M. A. J. Rodgers, *Ibid.* **101**, 3050 (1979).
[10a] P. B. Merkel and D. R. Kearns, *Ibid.* **94**, 1029 (1972); [b] P. R. Ogilby and C. S. Foote, *Ibid.* **105**, 3423 (1983); [c] J. R. Hurst, J. D. McDonald and G. B. Schuster, *Ibid.* **104**, 2065 (1982).
[11] A. A. Gorman, I. R. Gould and I. Hamblett, *Ibid.* **104**, 7098 (1982).
[12a] N. J. Turro, M.-F. Chow and Y. Ito, *Ibid.* **100**, 3580 (1978); [b] N. J. Turro, Y. Ito, M.-F. Chow, W. Adam, O. Rodriguez and F. Yany, *Ibid.* **99**, 5836 (1977).
[13a] N. J. Turro, V. Ramamurthy, K. C. Liu, A. Krebs and R. Kemper, *Ibid.* **98**, 6758 (1976); [b] C. Trindle and E. A. Holevi, *Int. J. Quantum Chem. Quantum Bio. Sym.* **5**, 281 (1978); [c] K. Okubo and H. Sato, *Bull. Chem. Soc. Jpn* **53**, 533 (1980); [d] G. D. Mendenhall, *Photochem. Photobiol.* **28**, 475 (1978).
[14] A. Krebs and H. Schmalstieg, University of Hamburg, unpublished results.
[15] H. Colberg, A. Krebs and N. J. Turro, unpublished results.
[16] G. Wittig and S. Fischer, *Chem. Ber.* **105**, 3542 (1972).
[17] G. Hefferon, Ph.D. Dissertation, Columbia University (1980).
[18a] J. Rigaudy, J. Guillaume and D. Maurette, *Bull. Soc. Chim. Fr.* 144 (1971); [b] H. H. Wasserman, J. Scheffer and J. L. Cooper, *J. Am. Chem. Soc.* **94**, 4991 (1972).
[19] N. J. Turro, M.-F. Chow and J. Rigaudy, *J. Am. Chem. Soc.* **103**, 7218 (1981).
[20a] P. Atkins, *Chem. Br.* **12**, 214 (1976); [b] A. Buchachenko, *Russ. Chem. Rev.* **45**, 375 (1976).
[21] A. Berndt, H. Fischer and H. Paul, *Magnetic Properties of Free Radicals*, Vol. 9b, Landoldt-Bornstein, New Series. Springer, New York (1977).